Article:
Xue, S., Chu, W.Q., Zhu, Z.Q. et al. (2016) Iron loss calculation considering temperature influence in non-oriented steel laminations. IET Science, Measurement & Technology, 10 (8). pp. 846-854. ISSN: 1751-8822

https://doi.org/10.1049/iet-smt.2016.0112

Iron Loss Calculation Considering Temperature Influence in Non-Oriented Steel Laminations

Shaoshen Xue [1*], W. Q. Chu [2], Z.Q. Zhu [1], Jun Peng [2], Shuying Guo [2], and Jianghua Feng [2]
[1] Department of Electronic and Electrical Engineering, University of Sheffield, Mappin Street, Sheffield, UK
[2] CSR Zhuzhou Institute Co. Ltd, Shidai Road, Shifeng District, Zhuzhou, Hunan, China
[*] sxue4@sheffield.ac.uk

Abstract: In this paper, the temperature influence on iron loss of non-oriented steel laminations is investigated. The iron loss variation under different flux densities, frequencies and temperatures is systematically measured and analysed by testing two typical non-oriented steel laminations, V300-35A and V470-50A. The iron loss variation with temperature is almost linear in the typical operating temperature range of electrical machines. Furthermore, the varying rate of iron loss with temperature varies with flux density and frequency. A coefficient which can fully consider the temperature influence is introduced to the existing iron loss model to improve the iron loss prediction accuracy. The predicted and measured results show that the temperature influence on the iron loss can be effectively considered by utilizing the improved model, i.e. the prediction accuracy of the improved iron loss model remains constant, even when the temperature varies significantly. A potential simplification of this improved model is also discussed in this paper.

1. Introduction

In electrical machines, iron loss is one of the major losses and its accurate prediction is essential for the evaluation of efficiency, temperature distribution, cooling requirements, and PM demagnetization etc. However, iron loss is one of the most difficult losses to predict accurately in electrical machines.

The first expression for the iron loss in ferromagnetic materials was developed by Steinmetz [1], where the iron loss is a sum of hysteresis loss and eddy current loss. In [2], a third term in the iron loss expression is introduced by Pry and Bean. The iron loss is separated into hysteresis loss, classical loss and excess loss. By improving the modelling of the excess loss, a new iron loss model is proposed by Bertotti et al. in [3] and [4]. Since the Bertotti model has good theoretical background, it has evolved into many different forms and is widely used for iron loss predictions [5]-[12]. However, it is concluded in [13] that the contributions of classical loss and excess loss cannot be separated by an Epstein frame or a ring specimen test. Alternatively, a new two-term approach is developed in [13], where the classical loss and excess loss in Bertotti's three-term model are combined into a global eddy current loss. Since this two-term model is easy to implement and has a reasonable accuracy, it is widely used in electrical machine design and optimization

[14]-[22]. All the iron loss models in [1]-[22] are based on constant coefficients. However, the iron loss coefficients change with the flux density and the frequency [23]. Therefore, in [24] and [25], iron loss models containing variable hysteresis and eddy current loss coefficients are developed. These models are used for the iron loss predictions in [26], [27], and [28].

It should be noted that none of the iron loss models in [1]-[28] consider the influence of temperature on the iron loss. The iron loss is predicted based on the measured iron loss curves, generally at room temperatures between 20ºC and 25ºC. However, the actual temperatures in stator and rotor cores vary significantly and could reach 100ºC or even higher [31]. More importantly, the iron loss can be significantly influenced by the temperature. In [29] and [30], the temperature influence on the iron loss of ferrite cores for power electronic applications is investigated and modelled. For electrical machine applications, the temperature influence on the initial magnetizing curve, the *B-H* hysteresis loops and the total iron loss of Ni-Fe laminations, are experimentally investigated in [31]. However, only the temperature influence on the magnetizing curve and torque performance is considered in the finite element (FE) simulations. In [32], the temperature dependency on iron loss of oriented silicon steels are experimentally confirmed. In [33], it is experimentally verified that the saturation flux density, permeability and iron loss of 35A360 Si-Fe laminations can be significantly influenced by the temperature. However, no further analyses and models are presented in [32] or [33]. In [34], the temperature influence on the resistivity of steel laminations is considered, the temperature influence on eddy current loss is then modeled by introducing a temperature dependent resistivity. However, the temperature influence on hysteresis loss is not taken into account while, as confirmed experimentally in [33] and [45], the hysteresis loss can be significantly influenced by temperature. Therefore, the model presented in [34] is not very accurate, especially considering the high flux density leading to a more significant variation of hysteresis loss with an increase in temperature.

The aim of this paper is to develop an iron loss model which considers the temperature influence on both hysteresis loss and eddy current loss as well as ensuring a good accuracy, while keeping the model simple and practical. In this paper, the iron loss variations of non-oriented Si-Fe steel laminations with the flux density, frequency and temperature are systematically measured. In order to obtain general conclusions, two typical non-oriented Si-Fe steel laminations, i.e. 0.35mm thick V300-35A and 0.5mm thick V470-50A, are investigated. The properties of V300-35A and V470-50A are shown in Table 1. This paper is organized as follows. In Section 2, the iron loss measuring method and test rig are presented. In Section 3, the measured iron loss at different flux densities, frequencies and temperatures is systematically analyzed. In Section 4, the predicted results of existing iron loss models are compared with the measured results. An improved iron loss model considering the influence of temperature on both hysteresis and eddy current losses is developed in Section 5. In Section 6, in order to evaluate the effectiveness of the improved iron loss model, the prediction

accuracies of existing and improved iron loss models are compared. A potential simplification of the improved model is discussed in Section 7.

Table 1 Properties of V300-35A and V470-50A

	V300-35A	V470-50A
Silicon content	2.5%	1.5%
Resistivity (40°C)	5.36×10^{-7} Ω m	4.02×10^{-7} Ω m
Resistivity (100°C)	5.82×10^{-7} Ω m	4.37×10^{-7} Ω m

2. Iron Loss Measurement

There are many methods to measure iron loss in steel laminations, such as, the Epstein frame test [36], the ring specimen test [37], and the single strip test [38] [39]. Comparisons between these iron loss measuring methods are carried out in [37], [40], [41] and [42]. The ring specimen test involves a similar principle to the Epstein frame test but is much easier to implement. Hence, the ring specimen test has been widely used [29] [33] [43] [44]. In this paper, all of the iron loss results under different flux densities, frequencies and temperatures are measured by the ring specimen test. The measuring system is shown in Fig. 1.

The ring specimen is made of the laminations to be measured, which is then wound with two coils, i.e. the excitation and measuring coils. The excitation coil is connected to the power source to produce the designated flux density waveforms in the specimen. In order to exclude the influence of copper losses due to the internal resistance of the power source and the resistance of the excitation coil, an open-circuit measuring coil is tightly wound together with the excitation coil. Furthermore, the number of turns for the excitation and measuring coils is chosen to be the same. Thus, the instantaneous current of the excitation coil and the instantaneous voltage of the measuring coil are measured and recorded on the oscilloscope simultaneously. The field strength $H(t)$, iron loss P_{Fe}, and iron loss density p_{Fe} can be calculated as

$$H(t) = Ni(t)/l_{\text{eff}} \tag{1}$$

$$P_{\text{Fe}} = \int_0^T i(t)u(t)dt \Big/ T \tag{2}$$

$$p_{\text{Fe}} = P_{\text{Fe}}/(\rho V) \tag{3}$$

where N is the number of turns of the excitation and measuring coils, $i(t)$ is the instantaneous current of excitation coil. $u(t)$ is the instantaneous voltage of measuring coil. l_{eff} is the effective length of the ring specimen. T is the time period of the current and voltage. ρ and V are the mass density and the volume of the specimen respectively.

Since the magnetic permeability of the lamination is much higher than the permeability of air, the flux leakage is negligible. Also, the flux density can be treated as evenly distributed in the specimen since the specimen has a much bigger average radius than radial thickness. In order to support this, the field distribution when the average flux density in the ring is 1.70T is simulated by non-linear finite element analysis as shown in Fig. 2. It is shown that the difference between the maximum and minimum flux densities in the ring is < 3% of the average flux density. In this case, the flux density $B(t)$ in the lamination can be obtained as

$$B(t) = \int u(t)dt/NA \qquad (4)$$

where A is the effective cross sectional area of the ring specimen.

In actual test rigs, the ring specimen is made of wire cut non-oriented Si-Fe steel laminations. In order to reflect the general influence of temperature on the iron loss, two typical non-oriented Si-Fe steel laminations, i.e. 0.35mm thick V300-35A and 0.5mm thick V470-50A, are investigated. 0.35mm and 0.5mm are the most widely used non-oriented Si-Fe steel lamination thicknesses for electrical machine applications. The excitation coil is made of Litz wire with a relatively large total conductor cross-section. The resistance of the excitation coil is 0.04Ω. Due to negligible voltage on the resistance, the flux density in the ring specimen and the induced voltage from the measuring coil are sinusoidal, even when the excitation current is non-sinusoidal. This can be seen in Fig. 3, especially so when the flux density is high due to the nature of non-linear soft magnetic materials. The excitation coil is powered by a California Instrument 4500iL power supply, whose maximum output voltage and current is 150V/30A RMS with an output frequency range of between 45Hz and 5kHz. The dimensions of the ring specimen and the coil number of turns are specially designed and given in Table 2 in order to cover the flux density and frequency ranges specified in Table 3.

In order to investigate the influence of temperature on the iron loss, firstly, a K-type thermocouple is installed on the ring specimen to measure the temperature. Secondly, the iron loss is utilized to heat up the ring specimen to any designated temperature higher than the room temperature. It should be noted that the electromagnetic time constant is much smaller than the thermal time constant for this system. It only takes a few seconds to stabilize the voltage and current and record these on the oscilloscope. During this period, the change of temperature is so small that it can be neglected. Thus, iron loss under different temperatures can be obtained. This method is also used in [33]. Since the room temperature varies and the lamination temperature is much easier to be maintained constant when it is higher than the room temperature based on the test rig, the lowest lamination temperature is chosen to be 40ºC in this paper. Furthermore, tests were repeated several times at each test condition to reduce any error.

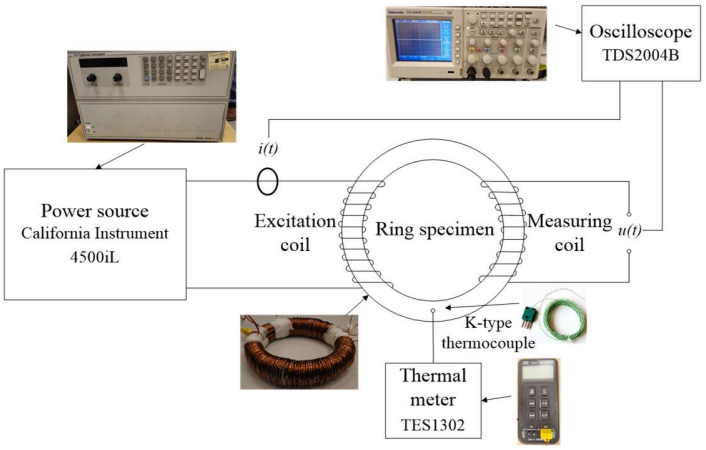

Fig. 1. *Schematic of iron loss test rig.*

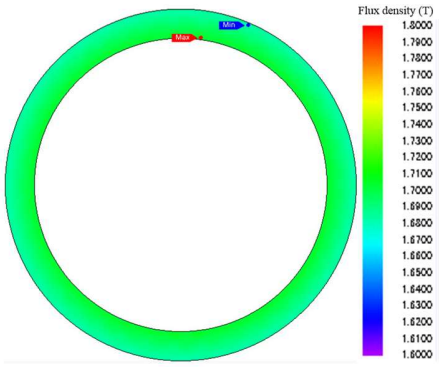

Fig. 2. *Non-linear FE predicted field distribution of ring specimen when average flux density is 1.7T.*

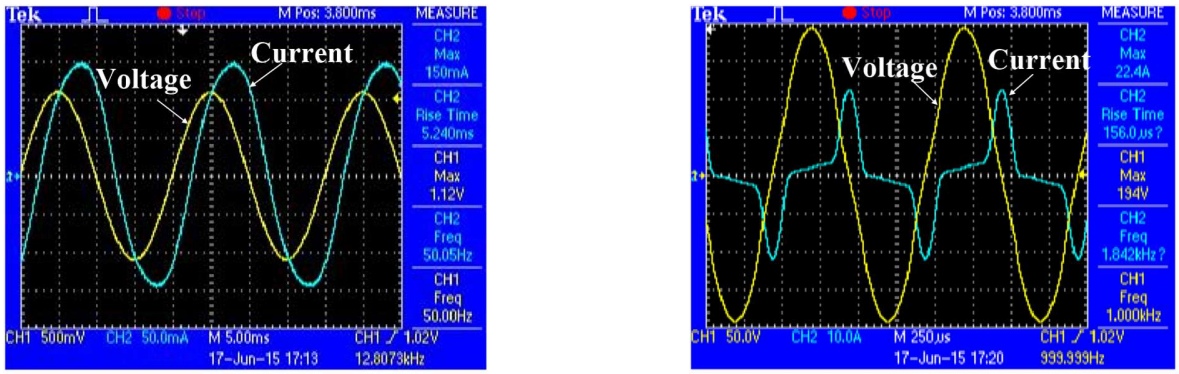

a b

Fig. 3. *Typical waveforms for measured currents of excitation coil and voltages of measuring coil.*

a B_m=0.2T and f=50Hz

b B_m=1.73T and f=1000Hz

Table 2 Parameters of ring specimen and coils

Outer diameter	150 mm
Inner diameter	125 mm
Total effective thickness	14 mm
Total layers of laminations	40 (for 0.35mm laminations) 28 (for 0.5mm laminations)
Number of turns for excitation and measuring coils	102

Table 3 Ring specimen iron loss test ranges

Flux density	0-1.8 T
Frequency	50-1000 Hz
Temperature	40-100 °C

3. Measured Iron Loss

Based on the method described in Section 2 and the test rig shown in Fig. 1, the iron loss under different flux densities, frequencies and temperatures is measured. In order to illustrate the iron loss variation more clearly, the investigation in this section is carried out in two steps. The iron loss variation with the flux density and the frequency at constant lamination temperature is analyzed first. The influence of temperature on the iron loss is then investigated separately.

3.1 Iron loss variation under constant lamination temperature

In order to illustrate the iron loss variation under a constant lamination temperature, the measured iron loss of V300-35A and V470-50A at 40ºC and 100ºC are shown in Fig. 4 (a) and (b), respectively. It is shown that the iron loss varies with the frequency and flux density in an identical pattern when the lamination temperature is 40ºC and 100ºC. The iron loss increases significantly when either the frequency or the flux density is higher. This variation pattern has been widely reported in [3], [4], [8] and [22] as well as modelled in [3] and [4]. However, the values of iron loss at 40ºC and 100ºC are different at the same flux density and frequency. This means that the iron loss in non-oriented steel laminations is influenced by the temperature. This will be investigated systematically later in this paper.

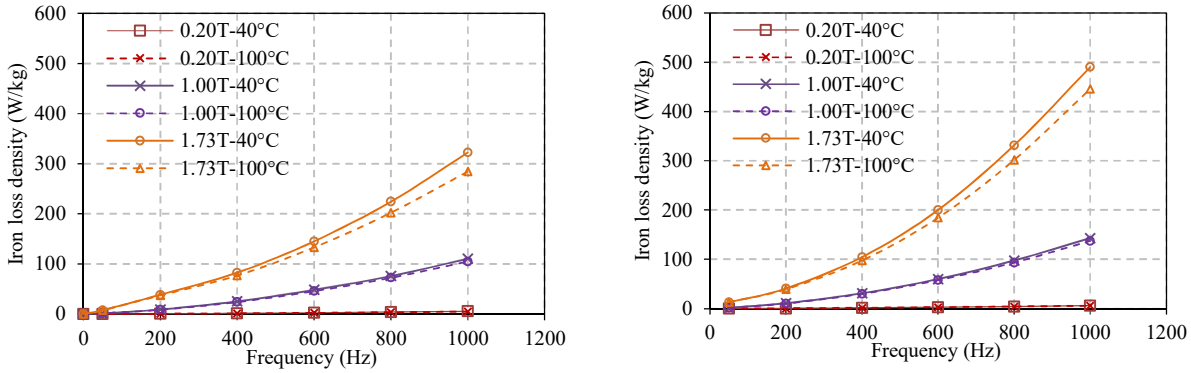

Fig. 4. *Measured iron loss density with frequency and flux density at lamination temperatures of 40°C and 100°C*

a V300-35A

b V470-50A

3.2 Influence of temperature on iron loss

In order to comprehensively investigate the influence of temperature, the iron loss variations with the temperature at various combinations of frequencies and flux densities in both V300-35A and V470-50A are measured, as shown in Fig. 5. For example, the yellow solid line with the star marker in Fig. 5 (a) is the iron loss of V300-35A lamination obtained when the flux density is 0.2T, at a frequency of 1000Hz and with a

lamination temperature change from 40°C to 100°C. It can be seen that the iron loss in both V300-35A and V470-50A laminations varies when the temperature rises across the whole test range. This is caused by the fact that the hysteresis loss and eddy current loss are dominated by the permeability and resistivity, which are influenced by temperature significantly. Furthermore, the iron loss varies almost linearly with the temperature rise. This is due to the fact that the permeability and conductivity of non-oriented steel laminations vary linearly between room temperature and 200°C, which has been experimentally confirmed in [33]. This linear temperature dependency of iron loss in other types of steel laminations is also reported in [35]. It should be noted that the temperature dependency of iron loss will be non-linear when the temperature is > 200°C [45]. However, electrical machines from normal industrial and domestic applications typically operate with a maximum temperature of < 120°C [31]. Therefore, the temperature dependency of iron loss can be considered as linear for this temperature range, which is much simpler but has a better accuracy. As shown in Fig. 5, the iron loss varies with temperature, with the amount of variation corresponding to different frequencies and flux densities. Taking the test results of the V300-35A lamination for instance, when the temperature increases from 40°C to 100°C, the iron loss at 1.73T and 1000Hz reduces by > 10% while the iron loss at 0.2T and 50Hz decreases by < 5%. This variation in the change of iron loss with temperature at different frequencies and flux densities will be investigated further in Section 5.

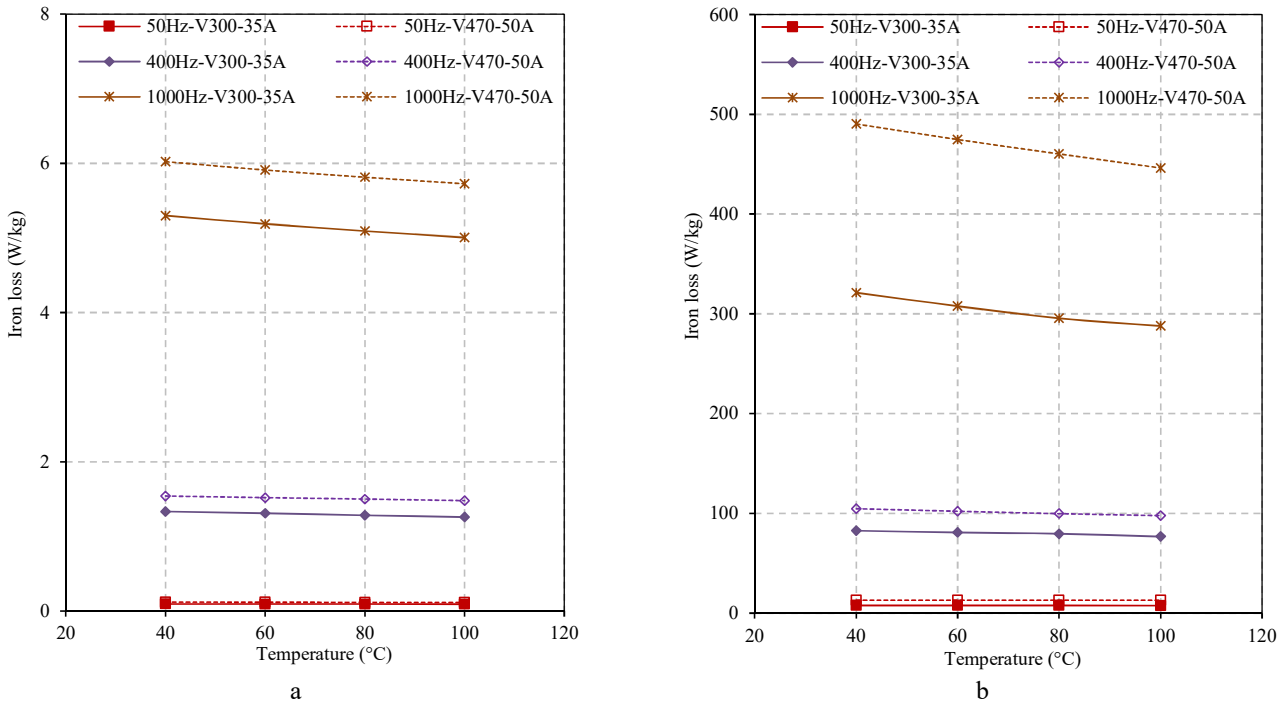

Fig. 5. *Measured iron loss variation with temperature, at different frequencies and flux densities in V300-35A and V470-50A*

a B_m=0.2T

b B_m=1.73T

4. Iron Loss Prediction by Existing Iron Loss Models

In this section, the accuracy of existing iron loss models is evaluated with and without considering the temperature influence. The differences between existing iron loss models are also highlighted.

According to the review of existing iron loss models in the introduction section, the iron loss models developed in [17] and [24] are two of the latest and most widely used models when the magnetic field is alternating sinusoidally. Hence, they are selected for the iron loss predictions in this section. The most accurate model will be selected for further investigation.

It should be noted that the influence of temperature on the iron loss is not considered in these iron loss models. Therefore, the coefficients of these iron loss models are calculated based on the measured iron loss results at a constant temperature. This temperature is chosen to be 40ºC in this paper, since the room temperature varies and the lamination temperature is much easier to maintain when it is higher than the room temperature.

The iron loss model with constant coefficients introduced in [17] is referred to as Model-1 in this paper and can be express as

$$p_{\mathrm{Fe}} = k_{\mathrm{h}} f B_{\mathrm{m}}^2 + k_{\mathrm{e}} f^2 B_{\mathrm{m}}^2 \qquad (5)$$

where p_{Fe} is iron loss density. f is the frequency. B_{m} is the peak value of alternating flux density. k_{h} and k_{e} are the hysteresis loss and eddy current loss coefficients respectively.

The iron loss model with variable coefficients introduced in [24] is referred to as Model-2 in this paper and can be express as

$$p_{\mathrm{Fe}} = k_{\mathrm{h}}(f, B_{\mathrm{m}}) f B_{\mathrm{m}}^2 + k_{\mathrm{e}}(f, B_{\mathrm{m}}) f^2 B_{\mathrm{m}}^2 \qquad (6)$$

where $k_{\mathrm{h}}(f, B_{\mathrm{m}})$ and $k_{\mathrm{e}}(f, B_{\mathrm{m}})$ are variable hysteresis loss and eddy current loss coefficients respectively.

Fig. 6 shows a comparison of the predicted iron loss and the measured iron loss in V300-35A and V470-50A laminations at different flux densities and lamination temperatures. Since these existing iron loss models do not consider the influence of temperature, the iron loss is predicted based upon the coefficients obtained at the specific temperature, which is 40ºC in this paper. It can be seen that when the temperature is constant at 40ºC, better accuracy can be achieved in both V300-35A and V470-50A laminations by utilizing Model-2 with the help of variable coefficients. Therefore, further investigation on the temperature influence on iron loss will be based on the iron loss Model-2 in this paper. However, it is shown in Fig. 6 that when the temperature increases from 40ºC to 100°C, the iron loss could vary significantly. The predicted iron loss by Model-2 cannot reflect this variation and remain unchanged when the temperature changes. Hence, the prediction accuracy of Model-2 varies significantly with the temperature.

This unstable prediction accuracy, which will be more clearly illustrated later in this paper, may mislead

the investigation and result in the wrong conclusions. Therefore, the iron loss model which considers the influence of temperature on the iron loss is desirable.

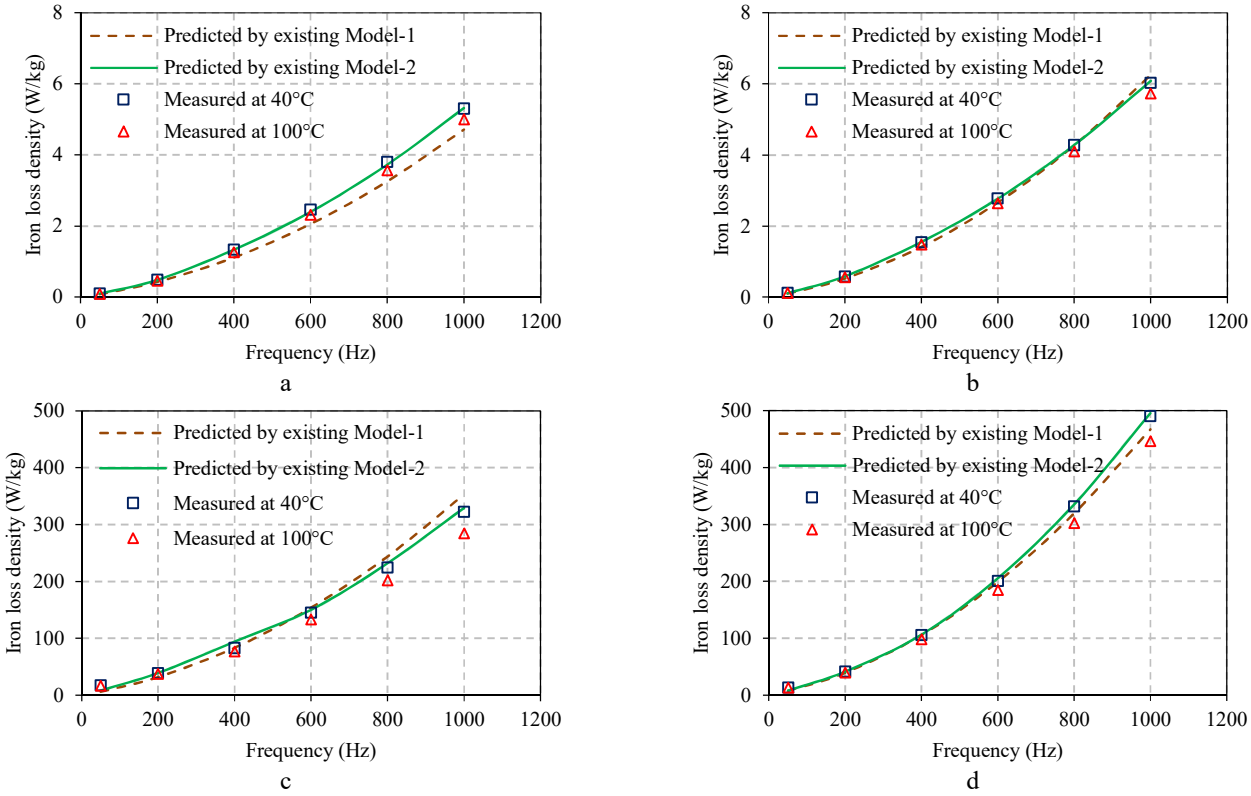

Fig. 6. *Measured iron loss at different temperatures and predicted iron loss by using existing models*

a B_m=0.2T, V300-35A

b B_m=0.2T, V470-50A

c B_m=1.73T, V300-35A

d B_m=1.73T, V470-50A

5. Iron Loss Calculation Considering Temperature Influence

As illustrated in Section 4, the iron loss can be influenced by temperature significantly. This is caused by the temperature dependency of eddy current loss and hysteresis loss. On one hand, the eddy current loss depends on the resistivity, which has an approximate linear dependency with temperature. On the other hand, as shown in [33] and [45], the permeability of non-oriented steel laminations fluctuates with temperature dramatically, which means the hysteresis loss is also significantly influenced by temperature. It is important to take temperature dependency of both the eddy current and hysteresis losses. However, the modelling of temperature dependency of the hysteresis loss is so complicated that would make the model impractical. Therefore in this section, the iron loss model which can consider the temperature dependency of eddy current loss while neglecting that of hysteresis loss is introduced at first. Secondly, an improved iron loss model which takes the temperature dependencies of both eddy current loss and hysteresis loss is presented. This improved iron loss model is also very easy to implement. The predicted and measured results are also

obtained and discussed in this section.

5.1 Iron loss prediction considering temperature coefficient of resistivity (Model-TCR)

As presented in [34], in order to take the temperature influence into account, one method is to consider the temperature dependency of eddy current loss while neglecting that of hysteresis loss. The eddy current loss coefficient is related to the electrical resistivity. The relationship between resistivity and temperature can be expressed as

$$\rho(T) = \rho_{T_0}[1 + \alpha(T - T_0)] \qquad (7)$$

where $\rho(T)$ is the resistivity at temperature T. ρ_{T_0} is the resistivity at the base temperature T_0. α is the temperature coefficient provided by manufacturers.

The iron loss model can be expressed as

$$p_{\mathrm{Fe},T} = k_{\mathrm{h}} f B_{\mathrm{m}}^2 + \frac{k_{\mathrm{e}}}{1 + \alpha(T - T_0)} f^2 B_{\mathrm{m}}^2 \qquad (8)$$

By applying (8) to the iron loss calculation, the predicted iron loss values vary with the temperature. The temperature influence on iron loss can be partly considered. However, since the temperature dependency of hysteresis loss is not taken into account, this model will be not very accurate. Fig. 7 shows the comparisons of the iron loss predicted by Model-2 (6) and Model-TCR (8) with measured iron loss at 100ºC. It is shown that the accuracy of Model-TCR is slightly better than that of Model-2 at 100ºC with the help of the temperature dependent resistivity. However, the improvement of accuracy with Model-TCR is limited. Furthermore, the predicted iron loss using Model-TCR will be overestimated and underestimated dramatically at different flux densities. This is caused by the different temperature dependencies of hysteresis losses, which are not taken into account in Model-TCR.

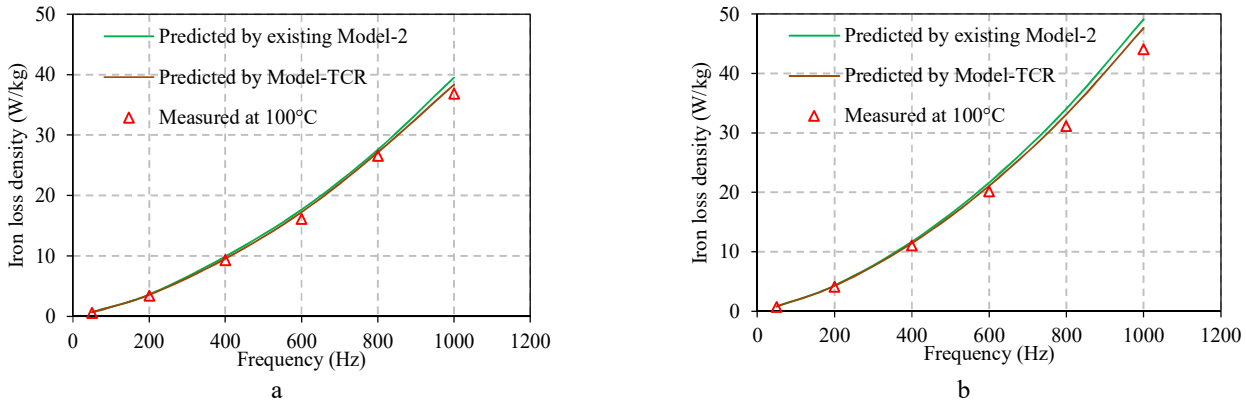

a b

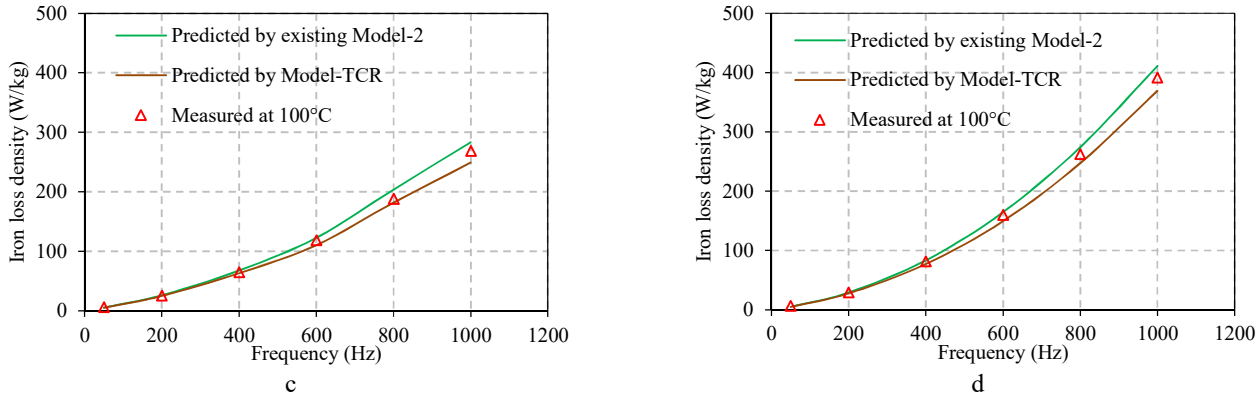

Fig. 7. *Comparison of iron loss predicted by Model-2 and Model-TCR with measured iron loss at 100°C*

a B_m=0.6T, V300-35A

b B_m=0.6T, V470-50A

c B_m=1.54T, V300-35A

d B_m=1.54T, V470-50A

5.2 Improved iron loss model

According to the investigation carried out in Section 5.1, it is necessary to take temperature dependency of both hysteresis and eddy current losses into account in order to achieve a good accuracy. However, the modelling of temperature dependency of hysteresis loss is so complicated that it would become impractical. In order to achieve a good accuracy while keeping the model easily implemented, a temperature dependent coefficient $k_t(f,T)$ is introduced to the total iron loss in this paper

$$p_{\mathrm{Fe},T} = k_t(f,T)p_{\mathrm{Fe,T_0}} \qquad (9)$$

where $p_{\mathrm{Fe},T}$ is the iron loss density at actual temperature T. $p_{\mathrm{Fe,T_0}}$ is the iron loss density at the base temperature T_0. $k_t(f,T)$ is the temperature coefficient representing the ratio of the iron loss when the temperature is T and T_0.

By applying (9) to the existing iron loss Model-2 (6), the iron loss model considering temperature influence can be expressed as

$$p_{\mathrm{Fe},T} = k_h(f,B_m,T)fB_m^2 + k_e(f,B_m,T)f^2B_m^2 \qquad (10)$$

Comparing (10) the iron loss model in this paper and (8) the iron loss model in [34], their differences can be summarized as: 1) In the iron loss model of [34], only the eddy current loss is influenced by the temperature. In this paper, both the hysteresis and eddy current losses are influenced by the temperature. 2) In the iron loss model of [34], the temperature coefficient is constant. In this paper, the temperature coefficient varies both with the temperature and frequency. 3) In the iron loss model of [34], the coefficients a for hysteresis loss and b for eddy current loss are constant. In this paper, the coefficients k_h for hysteresis loss and k_e for eddy current loss are functions of flux density and frequency. It is shown in [24] that the varying coefficients model has better accuracy than the constant coefficients model.

As shown in Fig. 5, the iron loss variation with temperature can be approximately considered to be linear, as has been illustrated in Section 3 when the flux density and frequency were constant. Thus, the temperature coefficient $k_t(f,T)$ can be expressed as

$$k_t(f,T) = 1 - (T - T_0)D \tag{11}$$

$$D = \frac{(p_{Fe,T_0} - p_{Fe,T_1})}{p_{Fe,T_0}(T_1 - T_0)} \tag{12}$$

where p_{Fe,T_1} is the iron loss density when the temperature is T_1. D is the iron loss varying rate per ºC. A positive value of D means that the iron loss decreases with temperature rise whilst a negative value of D indicates that the iron loss increases with temperature rise.

The values of D are obtained from the measured iron loss at two different temperatures when the frequency and flux density are fixed. By choosing T_0 = 40°C and T_1 = 100°C, the points in Fig. 8 (a) and (b) show the variations of D measured in the V300-35A and V470-50A laminations. It can be seen that D varies with the flux density differently depending on whether the frequency is low or high. This variation is caused by the difference in temperature dependency of hysteresis loss and eddy current loss with flux density and frequency, which has also been experimentally confirmed in [33], [45] and [46]. In order to ensure that the model is easy to implement, an engineering method is carried out to predict the values of D as follows. Firstly, the values of D are measured at several different flux densities and frequencies. Secondly, the values of D at each frequency are averaged, as shown in Fig. 8. Finally, the value of D at any frequency can be predicted by utilizing curve fitting to the averaged values, as shown by the dashed lines in Fig. 8.

Based on the foregoing method (9)-(12), an improved iron loss model is developed. The iron loss at any operating point in the test range can be predicted by measuring the iron loss at several points. In order to evaluate the improved iron loss model, the measured and predicted iron loss at 1.54T in V300-35A and V470-50A laminations when the temperature is 100°C is shown in Fig. 9. It can be seen from Fig. 9 that when the temperature changes to 100°C, the improved model can track the variations of iron loss precisely. Furthermore, the accuracy of the improved models is better than those of Model-TCR and Model 2.

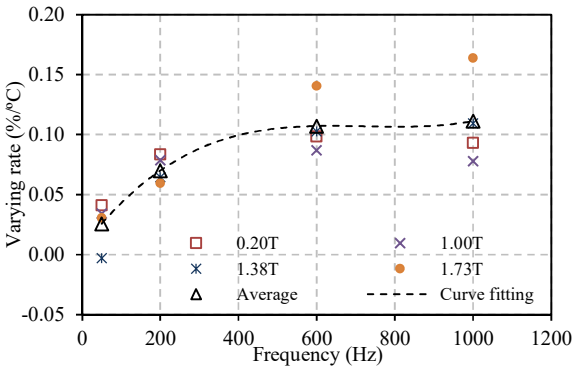

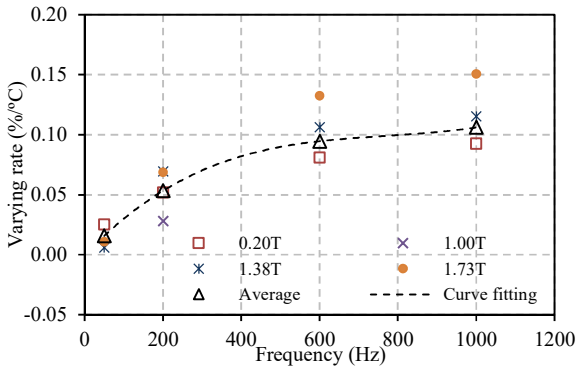

a b

Fig. 8. *Measured and calculated D at different flux densities*

a V300-35A

b V470-50A

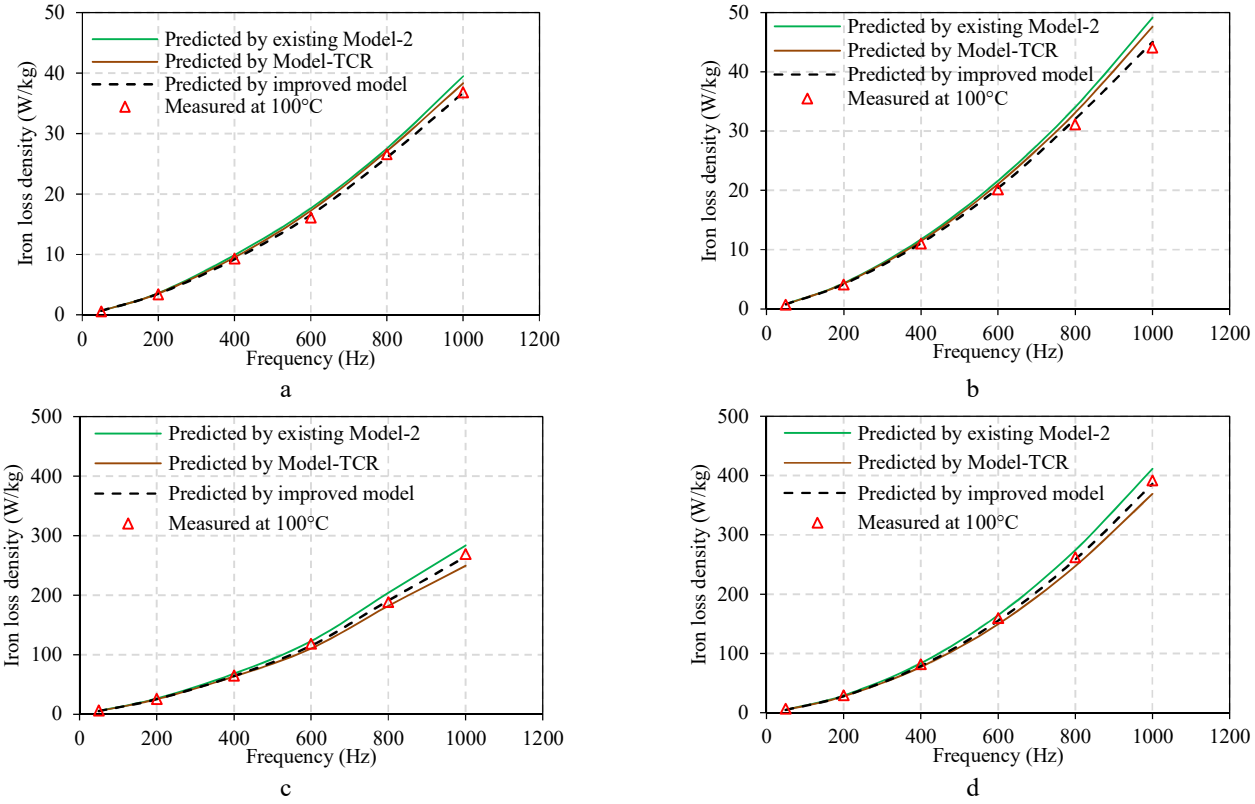

Fig. 9. *Comparison of iron loss predicted by Model-2, Model-TCR and improved model with measured iron loss at 100°C*

a B_m=0.6T, V300-35A

b B_m=0.6T, V470-50A

c B_m=1.54T, V300-35A

d B_m=1.54T, V470-50A

6. Iron Loss Model Validation

In order to evaluate the effectiveness of the iron loss model (10) at considering the influence of temperature on iron loss, predicted iron losses at different flux densities, frequencies and temperatures are analyzed and compared.

In order to demonstrate the difference between predicted values and measured values more clearly, the relative prediction error is introduced and defined as

$$err = (p_{\mathrm{Fe,Pre}} - p_{\mathrm{Fe,Mea}})/p_{\mathrm{Fe,Mea}} \qquad (13)$$

where $p_{\mathrm{Fe,Pre}}$ is the predicted iron loss density. $p_{\mathrm{Fe,Mea}}$ is the measured iron loss density.

With the help of the relative prediction error, it is much easier to judge whether the influence of temperature is considered effectively or not. The variation in relative prediction error with the temperature

will be greatly suppressed when the influence of temperature is considered effectively.

The comparison of relative prediction errors of existing Model-2, Model-TCR and improved model in both V300-35A and V470-50 laminations are shown in Fig. 10. It can be seen that the relative prediction errors of the existing iron loss Model-2 increase significantly when the temperature increases. This is due to the coefficients of the existing iron loss Model-2 being obtained at 40ºC. When the temperature rises, the prediction value is fixed, while the actual iron loss changes. The accuracy of Model-TCR has shown a slight improvement over that of Model-2, with the help of the temperature dependent resistivity. However, the prediction errors of Model-TCR still vary with the temperature significantly. Iron loss is overestimated or underestimate dramatically when the temperature is high. This is caused by the temperature dependency of hysteresis loss, which is not taken into account in Model-TCR. On the other hand, the improved model can predict the iron loss with a very low and stable relative prediction error when the temperature changes significantly. This means that the improved model has considered the influence of temperature on iron loss successfully.

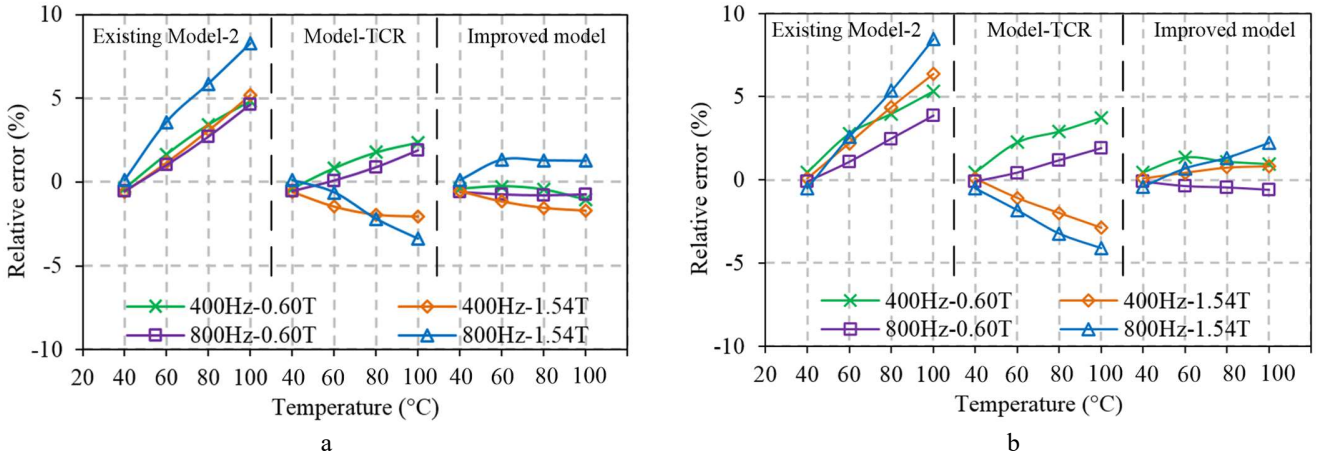

Fig. 10. *Relative prediction errors of existing Model-2, Model-TCR and improved model at different frequencies and flux densities in*

a V300-35A

b V470-50A

7. Discussions on a Potential Simplification of the Improved Model

It is shown in Fig.8 that the measured values of varying rate D of V300-35A and V470-50A are very similar. This is due to the fact that these materials are the same type of material, but with slightly different grades. Utilizing the feature of similar D, it is possible to predict the iron loss of one material under different temperatures based on the measured D of another similar material. This is illustrated in Fig. 11.

Both Figs. 11(a) and (b) compare two sets of iron loss predictions. In Fig. 11(a), the left set of data is the iron loss prediction error based on the original V300-35A data and the right set of data is based on values of D of V470-50A. In Fig. 11(b), the left set of data is the iron loss prediction error based on the original

V470-50A data and the right set of data is based on the value of *D* of V300-35A. It can be seen that the accuracy of iron loss predicted by the improved model based on the value of *D* of another similar lamination data are slightly degraded but still acceptable. This suggests that iron loss can be predicted by the improved model with reasonable accuracy even based on the measured value *D* of a similar material. In this case, measurements on only one grade of lamination can be used for temperature influence on iron loss in all the other grades of laminations within the same type, which further simplifies the implementation. However, it would be more convincing if the conclusion is confirmed by the measurements of a wider selection of laminations.

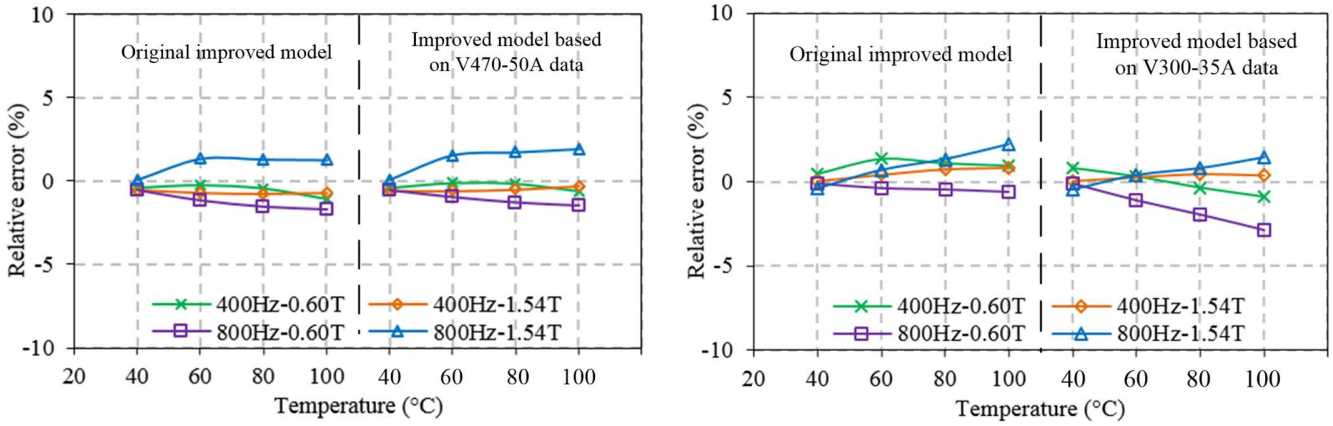

Fig. 11. *Relative prediction errors of original improved model and improved model based on other types of lamination data in*
a V300-35A
b V470-50A

8. Conclusions

In this paper, the temperature influences on iron loss of steel laminations is comprehensively investigated and considered in iron loss modeling. An improved iron loss model is proposed to fully consider the temperature influence on both the hysteresis and eddy current losses. It should be noted that both the hysteresis and eddy current losses are influenced by temperature. Although the temperature influence on the eddy current loss is easy to consider based on the resistivity variation, the temperature influence on the hysteresis loss can be significant and more complicated. The proposed iron loss model remains simple and easy to implement. It shows that the proposed iron loss model can predict iron loss with a good and stable accuracy when the temperature varies. The maximum calculation error of the suggested model is less than 3%. Based on this investigation, it is possible to model the iron loss considering the influence of temperature, which could be very useful in electromagnetic-thermal coupled finite element analyses. These modelling and electromagnetic-thermal coupled analyses are included in the work to be carried out in the near future.

9. References

[1] Steinmetz, C.P.: 'On the law of hysteresis', Trans. Amer. Inst. Elect. Eng., 1892, **9**, (1), pp. 3-64

[2] Pry, R., Bean, P.: 'Calculation of the energy loss in magnetic sheet materials using a domain model', J. Appl. Phys., 1958, **29**, (3), pp. 532-533
[3] Bertotti, G.: 'Physical interpretation of eddy current losses in ferromagnetic materials, I. Theoretical considerations', J. Appl. Phys., 1985, **57**, (6), pp. 2110-2117
[4] Bertotti, G.: 'General properties of power losses in soft ferromagnetic materials', IEEE Trans. Magn., 1988, **24**, (1), pp. 621-630
[5] Fiorillo, F., Novikov, A.: 'An improved approach to power losses in magnetic laminations under nonsinusoidal induction wave-form', IEEE Trans. Magn., 1990, **26**, (5), pp. 2904-2910
[6] Atallah, K., Zhu, Z.Q., and Howe, D.: 'An improved method for predicting iron losses in brushless permanent-magnet DC drives', IEEE Trans. Magn., 1992, **28**, (5), pp. 2997-2999
[7] Kowal, D., Sergeant, P., Dupre, L., and Vandenbossche, L.: 'Comparison of iron loss models for electrical machines with different frequency domain and time domain methods for excess loss prediction', IEEE Trans. Magn., 2015, **51**, (1), pp. 1-10
[8] Barriere, O., Appino, C., Fiorillo, F., Ragusa, C., Lecrivain, M., Rocchino, L., Ben Ahmed, H., Gabsi, M., Mazaleyrat, F. and LoBue, M.: 'Characterization and prediction of magnetic losses in soft magnetic composites under distorted induction waveform', IEEE Trans. Magn., 2013, **49**, (4), pp. 1318-1326
[9] Cossale, M., Krings, A., Soulard, J., Boglietti, A., and Cavagnino, A.: 'Practical investigations on cobalt-iron laminations for electrical machines', IEEE Trans. Ind. Appl., 2015, **PP**, (99), pp. 1
[10] Tang, Y., Zhu, F., Ma, J., and Ma, H., 'A practical core loss calculation method of filter inductors in PWM inverters based on the modified Steinmetz equation', in, IEEE Int. Symp. Ind. Electron., Istanbul, Turkey, Jun. 2014, pp. 386-391
[11] Krings, A., Nategh, S., Wallmark, O., and Soulard, J.: 'Influence of the welding process on the performance of slotless PM motors with SiFe and NiFe stator laminations', IEEE Trans. Ind. Appl., 2014, **50**, (1), pp. 296-306
[12] Krings, A., Cossale, M., Soulard, J., Boglietti, A., and Cavagnino, A.: 'Manufacturing influence on the magnetic properties and iron losses in cobalt-iron stator cores for electrical machines', in Proc. IEEE Energy Convers. Congr. Expo., Pittsburgh, USA, Sep. 2014, pp. 5595-5601.
[13] Boglietti, A., Cavagnino, A., Lazzari, M., and Pastorelli, M.: 'Predicting iron losses in soft magnetic materials with arbitrary voltage supply: an engineering approach', IEEE Trans. Magn., 2003, **39**, (2), pp. 981-989
[14] Seo, J., Kwak, S., Jung, S., Lee, C.G., Chung, T.K., and Jung, H.K. 'A research on iron loss of IPMSM with a frictional number of slot per pole', IEEE Trans. Magn., 2009, **45**, (3), pp. 1824-1827
[15] Zhu, S., Cheng, M., Dong, J.N., and Du, J.: 'Core loss analysis and calculation of stator permanent-magnet machine considering dc-biased magnetic induction', IEEE Trans. Ind. Electron, 2014, **61**, (10), pp. 5203-5212
[16] An, S., Sun, S., Zhong, Y., Ren, B., and Yang, H.: 'Reduction of switching loss for a transformer-based three-phase grid-connected inverter', in Power Electron. and Motion Control Conf., Harbin, China, Jun. 2012, pp. 1752-1755.
[17] Domeki, H., Ishihara, Y., Kaido, C., Kawase, Y., Kitamura, S., Shimomura, T., Takahashi, N., Yamada, T., and Yamazaki, K.: 'Investigation of benchmark model for estimating iron loss in rotating machine', IEEE Trans. Magn., 2004, **40**, (2), pp. 794-797
[18] Yamazaki K., and Matsumoto, M.: 'Characteristics analysis of induction motors by considering stress caused by shrink fitting', in Proc. IEEE Int. Electr. Mach. Drives Conf., Chicago, IL, USA, May 2013, pp. 1112-1118
[19] Yamazaki K., and Fukushima, W.: 'Loss analysis of induction motors by considering shrink fitting of stator housings', IEEE Trans. Magn., 2015, **51**, (3)
[20] Akaki, R., Takahashi, Y., Fujiwara, K., Matsushita, M., Takahashi, N., and Morita, M.: 'Effect of magnetic property in bridge area of IPM motors on torque characteristics', IEEE Trans. Magn., 2013, **49**, (5), pp. 2335-2338
[21] Yamazaki K., and Kanou, Y.: 'Shape optimization of rotating machines using time-stepping adaptive finite element method', IEEE Trans. Magn., 2010, **46**, (8), pp. 3113-3116
[22] Yamazaki, K.: 'Torque and efficiency calculation of an interior permanent magnet motor considering harmonic iron losses of both the stator and rotor', IEEE Trans. Magn., 2003, **39**, (3), pp. 1460-1463
[23] Ionel, D.M., Popescu, M., Dellinger, S.J., Miller, T.J.E., Heideman, R.J., and McGilp, M.I.: 'On the variation with flux and frequency of core loss coefficients in electrical machine', IEEE Trans. Ind. Appl., 2006, **42**, (3), pp. 658-666
[24] Ionel, D.M., Popescu, M., McGilp, M.I., Miller, T.J.E., Dellinger, S.J., and Heideman, R.J. 'Computation of core losses in electrical machines using improved models for laminated steel', IEEE Trans. Ind. Appl., 2007, **43**, (6), pp. 1554-1564

[25] Mthombeni T.L., and Pillay, P.: 'Physical basis for the variation of lamination core loss coefficients as a function of frequency and flux density', IEEE Ind. Electron. 32nd Annu. Conf., Paris, France, Nov. 2006, pp. 1381-1387
[26] Boglietti, A., Cavagnino, A., Ionel, D.M., Popescu, M., Staton, D.A., and Vaschetto, S., A general model to predict the iron losses in PWM inverter-fed induction motors', IEEE Trans. Ind. Appl., 2010, **46**, (5), pp. 1882-1890
[27] Popescu, M., Ionel, D.M., Boglietti, A., Cavagnino, A., Cossar, C., and McGilp, M.I.: 'A general model for estimating the laminated steel losses under PWM voltage supply', IEEE Trans. Ind. Appl., 2010, **46**, (4), pp. 1389-1396
[28] Choi, W., Li, S., and Bulent, S.: 'Core loss estimation of high speed electric machines: An assessment', IEEE Ind. Electron. Society 39th Annu. Conf., Vienna, Austria, Nov. 2013, pp. 2691-2696
[29] Wilson, P. R., Ross, J. N., and Brown, A. D.: 'Simulation of magnetic component models in electric circuits including dynamic thermal effects', IEEE Trans. Power Electron., 2002, **17**, (1), pp. 55-65
[30] Raghunathan, A., Melikhov, Y., Snyder, J., and Jiles, D.: 'Modeling the temperature dependence of hysteresis based on Jiles-Atherton theory', IEEE Trans. Magn., 2009, **45**, (10), pp. 3954-3957
[31] Krings, A., Mousavi, S. A., Wallmark, O. and Soulard, J.: 'Temperature influence of NiFe steel laminations on the characteristics of small slotless permanent magnet machines', IEEE Trans. Magn., 2013, **49**, (7), pp. 4064-4067
[32] Foster, K.: 'Temperature-dependence of loss separation measurements for oriented silicon steels', IEEE Trans. Magn., 1986, **22**, (1), pp. 49-53
[33] Takahashi, N., Morishita, M., Miyagi, D., and Nakano, M.: 'Examination of magnetic properties of magnetic materials at high temperature using a ring specimen', IEEE Trans. Magn., 2010, **46**, (2), pp. 548-551
[34] Chen, J., Wang, D., Cheng, S., Wang. Y., Zhu, Y., Liu, Q.: 'Modeling of temperature effects on magnetic property of nonoriented silicon steel lamination', IEEE Trans. Magn, 2015, **51**, (11), pp. 1-4
[35] Nakahara, M., and Wada, K.: 'Analysis of hysteresis and eddy-current losses for a medium-frequency transformer in an isolated DC-DC converter', Power Electro. Conf. 2014 Int., Hiroshima, Japan, May, 2014, pp. 2511-2516
[36] 'Methods of measurement of the magnetic properties of electrical steel strip and sheet by means of an Epstein frame', International Standard IEC 60404-2:2008.
[37] Boglietti, A., Cavagnino, A., Ferraris, L., and Lazzari, M.: 'The annealing influence onto the magnetic and energetic properties in soft magnetic material after punching process', IEEE Electric Mach. and Drives, Madison, USA, Jun. 2003, pp. 503-508
[38] Moses A.J., and Shirkoohi, G.H.: 'Iron loss in non-oriented electrical steels under distorted flux conditions', IEEE Trans. Magn., 1987, **23**, (5), pp. 3217-3220
[39] Pfutzner, H., and Schonhuber, P.: 'On the problem of the field detection for single sheet testers', IEEE Trans. Magn., 1991, **27**, (2), pp. 778-785
[40] Moses, A., and Hamadeh, S.: 'Comparison of the Epstein-square and a single-strip tester for measuring the power loss of nonoriented electrical steels', IEEE Trans. Magn., 1983, **19**, (6), pp. 2705-2710
[41] Espíndola, A., Tristão, F., Schlegel, J.P., Batistela, N.J., Sadowski, N., Kuo-Peng, P., Rigoni, M.: 'Comparison of iron losses evaluations by different testing procedures', Elect. Mach. 2010 XIX Int. Conf., Rome, Italy, Sept. 2010, pp. 1-4
[42] Krings, A., and Soulard, J.: 'Experimental characterization of magnetic materials for electrical machine applications', IEEE Elect. Mach. Design, Control and Diagnosis Workshop, Torino, Italy, Mar. 2015, pp. 85-89
[43] Muhlethaler, J., Biela, J., Kolar, J.W., and Ecklebe, A.: 'Core losses under the DC bias condition based on Steimetz parameters', IEEE Trans. Power Electron., 2012, **27**, (2), pp. 953-963
[44] Rodrigues L.K., and Jewell, G.W.: 'Model specific characterization of soft magnetic materials for core loss prediction in electrical machines', IEEE Trans. Magn., 2014, 50, (11), pp. 1-4
[45] Takahashi, N., Morishita, M., Miyagi, D., and Nakano, M.: 'Comparison of magnetic properties of magnetic materials at high temperature', IEEE Trans. Magn., 2011, **47**, (10), pp. 4352-4355
[46] Saito, T., Takemoto, S., and Iriyama, T.: 'Resistivity and core size dependencies of eddy current loss for Fe-Si compressed cores', IEEE Trans. Magn., 2005, **41**, (10), pp. 3301-3303